Journal of Environmental Radioactivity 270 (2023) 107292

Contents lists available at ScienceDirect

Journal of Environmental Radioactivity

journal homepage: www.elsevier.com/locate/jenvrad

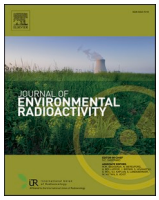

Examining the residual radiological footprint of a former colliery: An industrial nuclear archaeology investigation

Emily Parker [a], Matthew Ryan Tucker [a], Ilemona Okeme [b], Erin Holland [a], Dean T. Connor [c], Omer Mohamed [d], Peter G. Martin [a,*], Tom B. Scott [a]

[a] Interface Analysis Centre, School of Physics, HH Wills Physics Laboratory, University of Bristol, Tyndall Avenue, Bristol, BS8 1TL, UK
[b] University of Cardiff, School of Earth and Environmental Sciences, Cardiff University, Main Building, Park Place, Cardiff, CF10 3AT, UK
[c] National Nuclear Laboratory, Chadwick House, Birchwood Park, Warrington, Cheshire, WA3 6AE, UK
[d] School of Geographical Sciences, University of Bristol, University Road, Bristol, BS8 1SS, UK

A B S T R A C T

Nuclear industrial archaeology utilises radiation mapping and characterisation technologies to gain an insight into the radiological footprint of industrial heritage sites. Increased concentrations of naturally occurring radioactive materials at legacy mine sites are the result of elemental enrichment during coal mining and subsequent combustion. Public safety is of concern around these sites, and therefore, an increased understanding of their associated hazard is essential. Using coincident laser scanning and gamma detection technologies, this study sought to assess the radiological legacy of a coal mine located in Bristol, UK. From this, we can increase our understanding of the residual footprints associated with the local coal mining industry. Samples taken from inside the site were characterised using high resolution gamma spectrometry, wherein the radionuclide content and activities of samples were then quantified. An area of elevated low-level radioactivity was observed at and around buildings believed to belong to the colliery, while Th, U, and K are confirmed at the site from photopeak's of daughter radionuclides. Activities of the radionuclides K-40, U-238, and Th-232 were further quantified during subsequent laboratory analysis. Results highlight an enrichment of naturally occurring radionuclides when compared with global averages for unburned coal. Employing these techniques at further legacy sites would enable an increased understanding of the lasting traces of the coal mining industry, with a focus on NORM enrichment in residual fly ash.

1. Introduction

From a historic perspective, the Bristol coalfield was one of the earliest to be mined in the UK, providing fuel for heating homes, and power for Bristol's expanding industries. On the southern bank of the River Avon, in what is now central Bristol, a notable coal mining centre formed around the coal seams on land owned by the Smyth family (Bettey, 1978). This development attracted workers from the surrounding economically depressed agricultural areas, leading to the small town of Bedminster growing into a large suburb of Bristol, with over 70,000 inhabitants by 1884.

The Bristol and Somerset Coalfields are widespread below Bristol – with mining becoming prevalent throughout the 19th and early 20th centuries, accelerating the extraction of the resource that had been mined in the region for centuries prior. However, reports state that the coal is low grade, ashy, and seams were often narrow and subsequently low yield (Woodward, 1876; Ramsey, 2003). The demise of the industry at the beginning of the 20th century led to the closure of most of Bristol's working collieries, with the last closing its doors in 1963 (Ramsey, 2003). While coal production in the UK reached its peak in 1913, hundreds, if not thousands, of legacy mine sites remain scattered across the country (BGS, 2010).

Fly ash has historically been generated as a by-product of coal mining, through its use as fuel for the steam-engines employed to remove water from underground excavations. This fine-grain material often accumulates on the walls and floors of the surrounding infrastructure over the prolonged periods of time during operations. Alongside the commonly reported hazards associated with coal mining, the enrichment of potentially harmful elements in mine tailings, such as coal fly ash, is of particular concern. Toxic elements, such as arsenic and antimony are often concentrated in fly ash and can reach concentrations of up to 10 times that of the original mined coal (Tian et al., 2018). In addition to heavy metals, the combustion of coal also concentrates radionuclides into its end products - with fly ash and coal slag, therefore, containing heightened quantities of the naturally occurring radioactive materials (NORMs), including U, Th and K-40 and their associated radioactive daughter decay products/progeny. Concentrations of NORMs in fly ash have been seen to reach between 3 and 10 times that of

* Corresponding author.
E-mail address: peter.martin@bristol.ac.uk (P.G. Martin).

https://doi.org/10.1016/j.jenvrad.2023.107292
Received 4 October 2022; Received in revised form 6 June 2023; Accepted 1 September 2023
Available online 12 September 2023

those in the original precursor coal (Okeme et al., 2020). NORM concentrations at legacy mine sites have increased as a direct result of mining and are often referred to as Technologically Enhanced NORM, or TENORM (WNA, 2020).

Fly ashes and coal wastes are becoming increasingly valuable, especially those enriched in NORMs, as they are potentially rich resources for uranium recovery (Sun et al., 2016). Comparable with low-grade ore deposits in terms of yield, they are a potential source of uranium that doesn't require mining. As well as being enriched in radionuclides, fly ash is also often enriched in valuable metals, such as the rare earth elements (REEs) (Okeme et al., 2020). As these valuable metals are refractory and dense, they consequently typically sink to the bottom of mine tailings and accumulate in heightened concentrations at the base of a deposit. Because of this, fly ash hosts potentially economic deposits with little additional environmental impacts (Okeme et al., 2021). However, the enrichment of NORMs and trace elements in the remnants of coal mining pose health concerns for those living in close proximity to legacy mines. Radiation doses immediately at, or surrounding, such sites have the potential to exceed safe levels and should therefore be measured and quantified.

The range and concentration of elements in coal residues will depend heavily on the origin of the material and its relative mineralogy. The Lower Coal series of the Bristol and Somerset Coalfield outcrops extensively around south Bristol and specifically across the Bedminster area (Moore and Trueman, 1939). However, little information is readily available regarding the mineralogy of worked coal other than that the Lower Coal measures were the most valuable of the entire coalfield, with the coal derived from the Lower Coal measures primarily used in households, but also as coking (or steam) coal (Woodward, 1876).

The activity of remnant radionuclides at legacy mine sites can be quantified using radiation detectors, such as gamma detectors. A legacy coal mine in Bristol, UK, was chosen for the purpose of this study. Utilising portable GPS-integrated gamma-ray spectrometers, the site was mapped to determine the relative distribution, intensity, and energy of gamma-ray emitting radionuclides. Concurrently, the site was mapped with a handheld 3D Light Detection and Ranging (LiDAR) scanner to generate a cm-accurate point-cloud, which allowed correlation and calibration of radioactivity with specific physical features. Scrapings taken from inside the site, at the inside base of the old colliery chimney were subsequently analysed and characterised using High Purity Germanium (HPGe) gamma spectroscopy for direct comparison with ground-based data.

Numerous studies investigating radioactivity at active coal mines and coal-fired power plants are available, but studies into the radioactivity of legacy sites are limited. A study by Dowdall et al. (2004) investigated the lasting radiological impacts of the coal industry in the Arctic Ocean Island of Svalbard, determining a direct relationship between elevated radiation dose and areas of historic coal mining. The work detailed herein demonstrates a novel and highly accurate method for developing 3D radiation maps of legacy sites, with a view to providing important dosimetry information to underpin environmental safety assessments.

2. Study site

The subject of this study is Dame Emily Park, a community park located in Bedminster, Bristol. Now an open space for recreation, the park is located on the site of the old Dean Lane Colliery, a legacy pit mine that employed over 400 men and children at the peak of its production. Although the exact date of the commencement of operations is unknown, coal reserves began to run low at the start of the 20th century, with the colliery subsequently forced to close in 1906 (Ramsey, 2003). Following its closure, possession of the colliery and its land returned to the Smythe family, who donated it for public use (Ramsey, 2003). The site was cleared in 1910 and became a recreation ground, now known as Dame Emily Park (Lyes, 2002). Ordnance survey maps, as shown in Fig. 1, display the transition of the site from colliery (Fig. 1 (a)) to community park (Fig. 1(b)), where Dame Emily Park is now a valuable open space for Bristol, with skatepark, basketball courts, and community gardens (Ordnance Survey, 2013a, 2013b). It is unknown whether any land remediation works were conducted post-closure, but the shaft heads were covered (presumably infilled or blocked), and the bounding ground surface was topographically remodelled. The present-day skatepark is situated on the location of the former Pit Head, with a multi-purpose games area now atop what would have previously been the mines spoil heaps, as shown in the map of Fig. 1(a). Despite the renovation of the site, the old colliery chimney remains intact, attached to the Bristol South Swimming Baths, which was formerly the colliery bath house, used by the mines workers.

The Bedminster Great Vein, a thick coal seam of the Lower Coal series, was mined at the Dean Lane Colliery (Moore and Trueman, 1937). During operations, an explosive mixture of methane and other gases originating from coal seams, known as Firedamp, was a common problem when the Lower Coal series was exploited, often causing

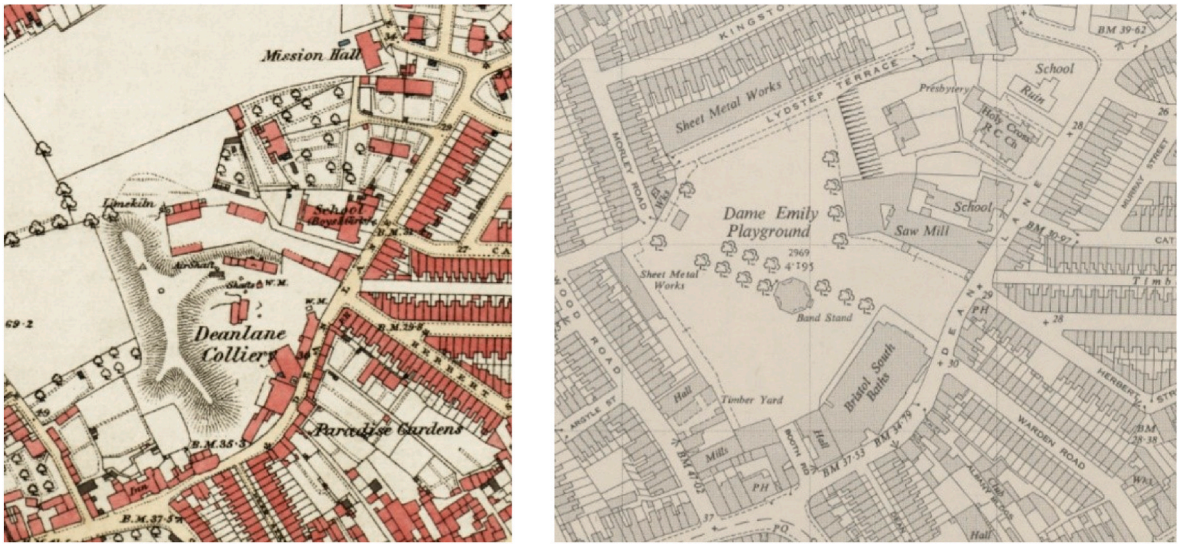

Fig. 1. Historic maps of the survey site. (a) as the Dean Lane Colliery in the 1844–1888 OS 25'' 1st Edition Map (Ordnance Survey, 2013a) and (b) as Dame Emily Park in the 1947–1965 OS National Grid Map (Ordnance Survey, 2013b). Both maps sourced from Know Your Place (2022).

harmful and substantial explosions at this site, as well as other collieries, across Bristol (Douet, 2016). Airborne coal dust was another commonplace problem in mines that frequently led to explosions, with a gas explosion at the site in 1886 leading to the death of 11 men (Ramsey, 2003). The active pumping of water to enable the working of seams that existed below the natural water table of the area was facilitated by (what was revolutionary at the time) steam-powered pumps fed with coal derived from the mine workings - with waste heat from the combustion used to warm the waters of the adjoining bath house. Over many years of operation, a substantial amount of waste fly ash would have been generated in the colliery's pump house.

The escape of NORMs and toxic metals into the atmosphere is of little concern at Dame Emily Park, where waste products of mining will remain in-situ until disturbed or removed. Furthermore, the quantity of residual material at the colliery is also low, so any identifiable quantities of such materials should be minimal. However, care was taken during this investigation when entering the buildings and disturbing residual material for the purposes of sampling. An increased understanding of the NORM content of the fly ash would enable a safety assessment for the site, to define whether additional safety measures should be emplaced.

3. Materials and methods

3.1. Ground-based surveys

The site survey combined gamma detection and 3D laser scanning technologies to produce a 3D overlay map, whereby gamma measurements were overlaid onto the 3D LiDAR plot to produce a comprehensive and accurately positioned radiation map, displaying the distribution of NORM across the former mine site. As the measurements are ground-based, they therefore display a high spatial resolution when compared with aerial surveys and are suitable for a site of such scale and accessibility. All the survey equipment was handheld and portable, whereby a single person can transport the entire system – with a second person ensuring consistent and accurate data collection, as well as safety throughout.

Initial transects of the site were undertaken, followed by further runs to supplement the data acquired. Supplementary runs covered more of the site and ran closer to the colliery buildings, affording a denser point-cloud. All data collected was loaded into the software CloudCompare for subsequent visualisation and interpretation (CloudCompare, 2015).

3.1.1. 3D Light Detection and Ranging (LiDAR)

LiDAR measures distance as a function of the time taken for an emitted laser pulse to be reflected from a surface and return to the unit (Vetter et al., 2019). 3D LiDAR scanners use rotating beams to disperse laser pulses in multiple directions (Vetter et al., 2019), whereby one pulse equals one point, and a collection of these points, called a point-cloud, produces a 3D model of the scene.

In this study, the 'Frontier' handheld 3D LiDAR scanner, developed by the Oxford Robotics Institute (ORI) was used. Alongside a 64 channel Ouster OS1 Lidar, the Frontier comprises an Inertial Measurement Unit (IMU) which can determine the platforms relative motion, orientation, and direction as the unit is moved, as well as allowing on-the-fly correction of the accumulating point-cloud, with the device resultantly producing point-clouds with centimetre accuracy (Ramezani et al., 2020). When undertaking the LiDAR survey, the practice of periodically returning to the same point to 'close loops' corrected for any drift in locational accuracy that would otherwise have occurred over time (Ren et al., 2019). The process of Simultaneous Localisation and Mapping (SLAM) allows for accurate location of regions of heightened radioactivity in context with their surroundings (Vetter et al., 2019).

3.1.2. Radiation detection and aggregation

Supplementing the Frontier scanner, four Hamamatsu Photonics Ltd C12137-01 gamma-ray spectrometers simultaneously recorded the radiation levels across the Dame Emily Park survey site. The four detectors were arranged at 90° separations (front, rear, left, and right) on a belt carried by the single operator, in an arrangement that enabled multi-directional radiation detection. This ensured that the detectors and LiDAR could be carried by the same person and could therefore record data simultaneously and at the same location. The detectors were therefore roughly 1 m above the ground, at a consistent height throughout data collection.

The detectors, each with a crystal size of 38 x 38 × 25 mm and weighing only 320 g, are compact and lightweight, making them ideal for individual handheld surveys. Each of the detectors comprise a Thallium-doped Caesium Iodide (CsI) scintillator and a Multi-Pixel Photon Counter (MPCC) (Hamamatsu, 2020). The detectors used have been modified by the manufacturer to increase their upper energy range (maximum) to 3 MeV (full range: 30 keV to 3 MeV), with a dose-rate measurement range of 0.01–100 μSv/hr (Hamamatsu, 2020). Now a staple of radiation detection and assay in Japan in response to the Fukushima Daiichi Nuclear Power Plant accident, the family of devices is now widely used – with energy resolution and dose-rate measurement errors of 8.5% and ±20%, respectively (Hamamatsu, 2020). The detectors each output a gamma spectrum every second, made up of 4096 energy-specific channels, with the spectra summed to provide counts per second (CPS) readings. A Raspberry Pi 4B single board computer is used to interface with the detectors, with spectral data sent over secure local WIFI to the Frontier sensor system.

The manufacturer of the detectors provides calibration information relating the specific channel number output from the device to the gamma energy detected, alongside the corresponding contributions per channel for dose (as pSv/photon). The relationship between channel number and gamma energy has been verified through measurements of sources with known emission peaks - with dose contributions also having been verified through measurement of a Cs-137 source of known activity, but further verification would be desirable to further reduce numerical uncertainties.

Interpolation of radiation measurements using the Kriging method was performed to infill missing results and produce a full coverage map of the site. The code used to produce the interpolated dataset was adapted from the code provided in West et al. (2021). Such a Kriging method utilises Poisson distributions to estimate and infill missing results, and is often favoured in radiation surveys, where the distribution of radiation from point sources is not always uniform (Zhao et al., 2019). Uncertainty in measurements increased with distance from collected data points, and points above a certain uncertainty threshold were removed to ensure confidence in the produced interpolation.

3.2. Sample collection and preparation

Two fine-grained 250 g fly ash samples were collected at the site and labelled C1 and C2, respectively. The samples were crushed using a pestle and mortar and oven dried at 100 °C for 30 min to extract any residual moisture from the already very fine and dry sample materials. Post-drying, the samples were pulverised, homogenised, and passed through a 250 μm wire mesh sieve.

To ensure secular equilibrium between decay products, prior to analysis, 200 g of each sample was placed into a snap-on lid re-useable re-entrant mini Marinelli beaker (from GA-MA Associates, USA) and left for 30 days. Polyvinyl chloride (PVC) tape wrapped around the seal of each beaker was used to ensure the beakers remained airtight. This prevented the escape of gaseous Rn-222 and Rn-220, maintaining secular equilibrium within the samples.

3.3. High resolution gamma-ray spectroscopy

A high-resolution P-type coaxial ORTEC, GEM-13180 high purity germanium (HPGe) detector was used to analyse the two samples obtained from the Dame Emily Park site (Ortec, 2020). The detector has a

10% relative efficiency, and a 1.71 keV resolution at 1.33 MeV (Co-60). To reduce any background contribution to photopeak intensity, the detector was shielded in a 10 cm wall lead covering lined with 2 mm copper and cadmium foils.

A detector energy calibration was performed using a high specific activity multi-nuclide point source (Model 7603, Eckert and Ziegler, 2007) with gamma-ray emission lines spanning the full range of the radionuclides of interest (40 keV–1,836 keV). An elementary efficiency calibration was performed using the IAEA certified reference material IAEA-385 (sea sediment) as a calibration source (IAEA, 2019). A more comprehensive efficiency calibration correction was not performed however, with measures taken into consideration to greatly reduce both the summing and matrix effects. The samples were placed at about 7 cm from the detector head, rather than being located directly over the detector head.

3.4. Activity concentration determination

When calculating the activity concentrations of U-238, Th-232, and K-40, the following equation was used, taking the ratio of radionuclide activity in the reference sample and in the fly ash sample.

Activity concentration:

$$A\left(Bqkg^{-1}\right) = \frac{N}{(\varepsilon.M.T.\gamma)} \quad (1)$$

where N is the background corrected net count, ε is the radionuclide photo peak efficiency, M is the mass of the sample in kg, T is counting time in seconds, and γ is the gamma yield of the radionuclide.

Activity concentrations of U and Th were determined by their relative gamma-emitting decay products, occurring in secular equilibrium. Secular equilibrium was confirmed in the Ra-226 series, and in Ra-228 and Th-228 respectively, using ratios of their respective decay products (~1). The activity of K-40 was calculated from its characteristic gamma emission energy of 1,461 keV.

The activity concentration of U-238 was determined via Ra-226 through the averaging of the activity concentrations of its decay products Pb-214 (352 keV) and Bi-214 (609 keV). Similarly, the activity concentrations of Ra-228 and Th-228 were determined from their decay products Ac-228 (911 keV) and Tl-208 (583 keV), respectively. The activity concentration of Th-232 was determined from the average value of the respective Ra-228 and Th-228 activity concentrations.

4. Results

4.1. 3D lidar

The resulting 3D point-cloud of the Dame Emily Park site is displayed in Fig. 2. Distinguishable on the point-cloud are the skate park, basketball courts and the old bath house building, including the colliery chimney, which can be seen in Fig. 2(c), marked with the white arrow.

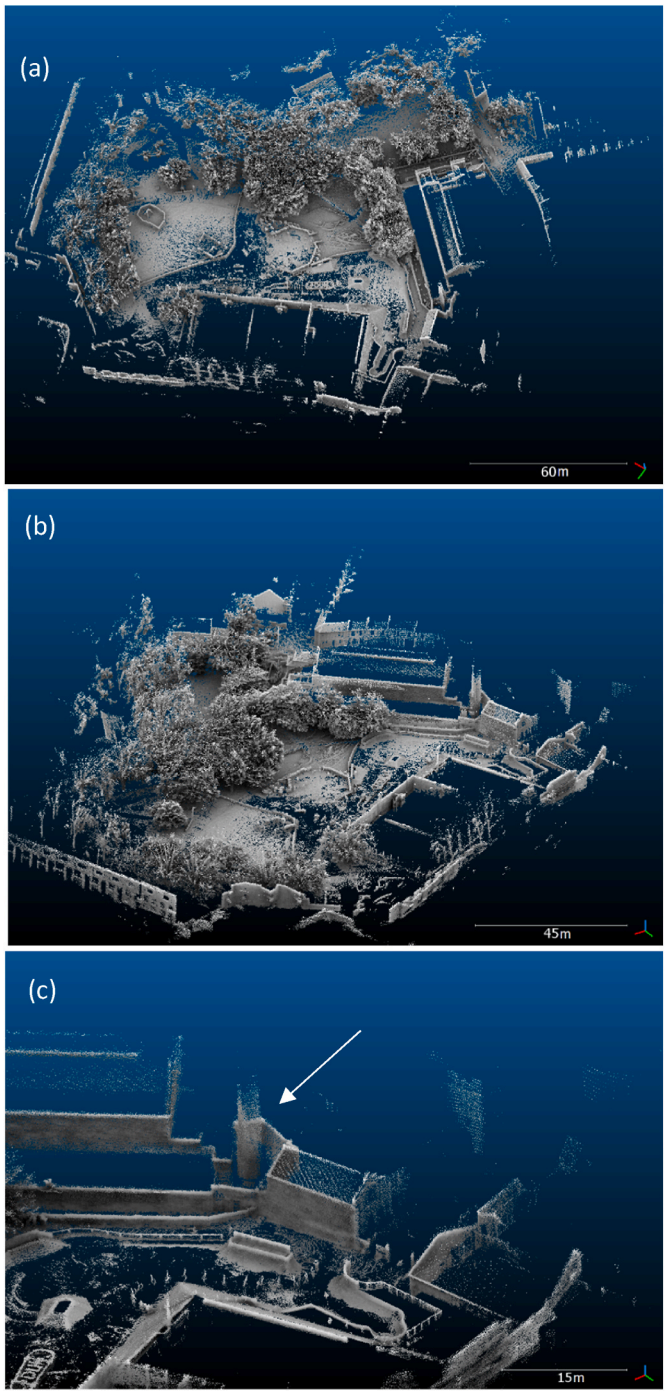

Fig. 2. (a) and (b) 3D point-cloud of Dame Emily Park, produced in the CloudCompare™ software, (c) Zoomed-in view of the colliery buildings, labelled with white arrows. The scale bar is in metres.

4.2. Radiation distribution

Radiation mapping outputs from all four detectors were overlaid onto the laser-generated point-cloud using the CloudCompare™ software (CloudCompare, 2015). The number of mapped LiDAR points has been reduced in the plots to increase the ease of viewing gamma results. The distribution of gamma radiation across the site is seen in Fig. 3, in which radiation can be seen to increase at and around the buildings to the right of the park. The results of this study highlight that locations of heightened radiation, as observed by gamma spectrometers, coincide with the location of the collieries remaining infrastructure. Radiation levels, in CPS, are low for most of the site (<90 CPS). The highest recorded radiation intensity at the site was 0.18 $\mu Svhr^{-1}$, with the lowest at 0.01 $\mu Svhr^{-1}$. An average dose value of 0.05 $\mu Svhr^{-1}$ across all four detectors for the survey area was calculated. The standard deviation of data from all four gamma detectors is low, representing a high percentage of measurements clustering around this average. These activity (and consequently dose-rate) levels, in terms of corresponding dose, were observed to be well below levels that which would constitute a regulatory or health concern. Field results have confirmed the presence of heightened radioactivity in the immediate area surrounding the colliery chimney, but further 'ground-truth' laboratory analysis of samples collected from inside the chimney was required to pinpoint the exact NORMs producing radiation peaks (see Fig. 4).

Differences in measured CPS were observed between the four

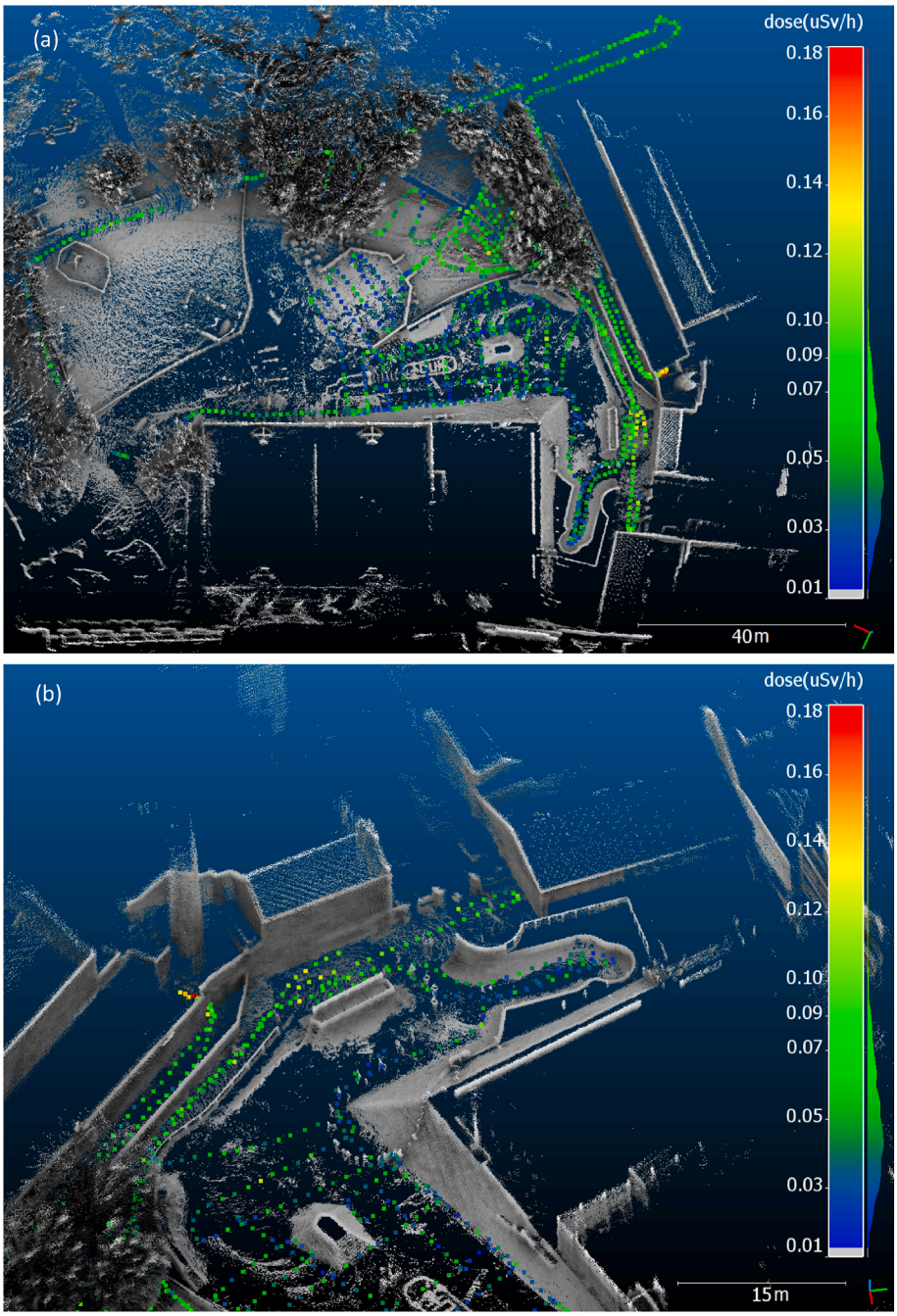

Fig. 3. (a) 3D point-cloud with overlaid gamma measurements. (b) Zoomed-in view of the colliery chimney, where radiation intensity is at its highest across the site, at the location labelled by the white arrow.

detectors. However, each exhibited elevated count rates at the same locations. The differences in recorded radiation arise from varying detector-to-source distances and the differential attenuation that the radiation experiences, through both the operator's body and in air.

Interpolating our results using the Kriging method helped to better visualise the gradational distribution of radiation across the site (West et al., 2021). Gamma measurements from the initial run across the site were interpolated to produce the map shown in Fig. 5. Two small areas of elevated radioactivity were determined, located proximal to the chimney building. The area closest to the chimney is enclosed by bricks, leading to some suggestion that the increased readings may instead be due to proximity to this material. However, the measurements closest to the chimney are observably higher.

The data capture took approximately 1 h in total, enabling complete radiological and 3D capture of the site very rapidly, with basic point-cloud and radiation data being viewed in real-time as the survey progressed. Such real-time data output enabled the survey to be conducted in a more intuitive manner, as areas of elevated radioactivity could be determined on-the-fly and given greater (and immediate) scrutiny during data capture.

4.3. Gamma-ray spectroscopy

An example gamma spectrum of one of the ground-truth samples is shown in Fig. 6. Labelled on the spectra are isotopes of the Th-228 and U-238 decay chains, alongside K-40 - also shown are photopeak emissions of Pb, Tl, Bi, and Ac. Further daughter isotopes of the U and Th decay series in addition those labelled are also present, but due to low

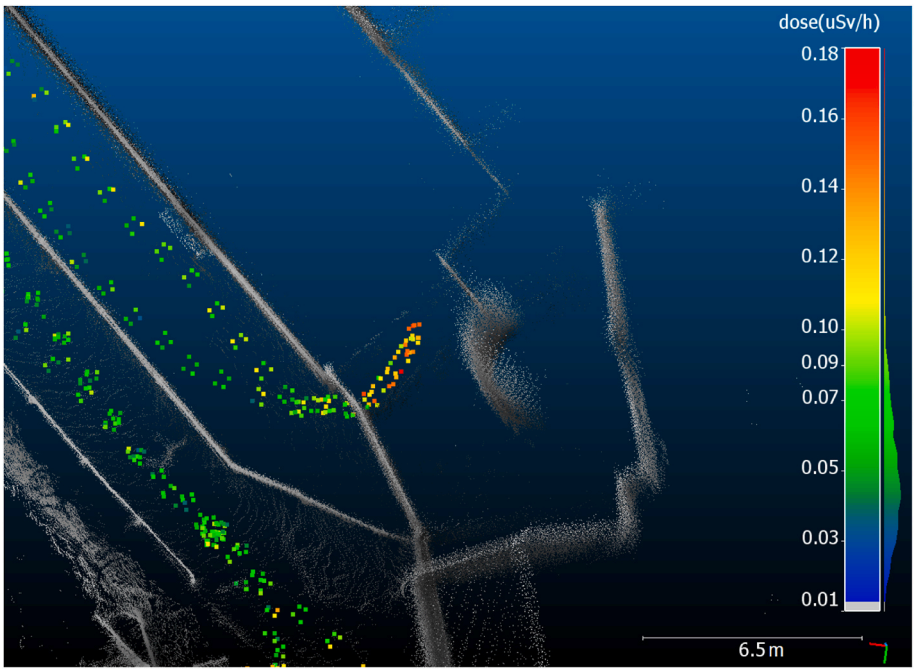

Fig. 4. Measurements closest to the chimney, showing elevated counts.

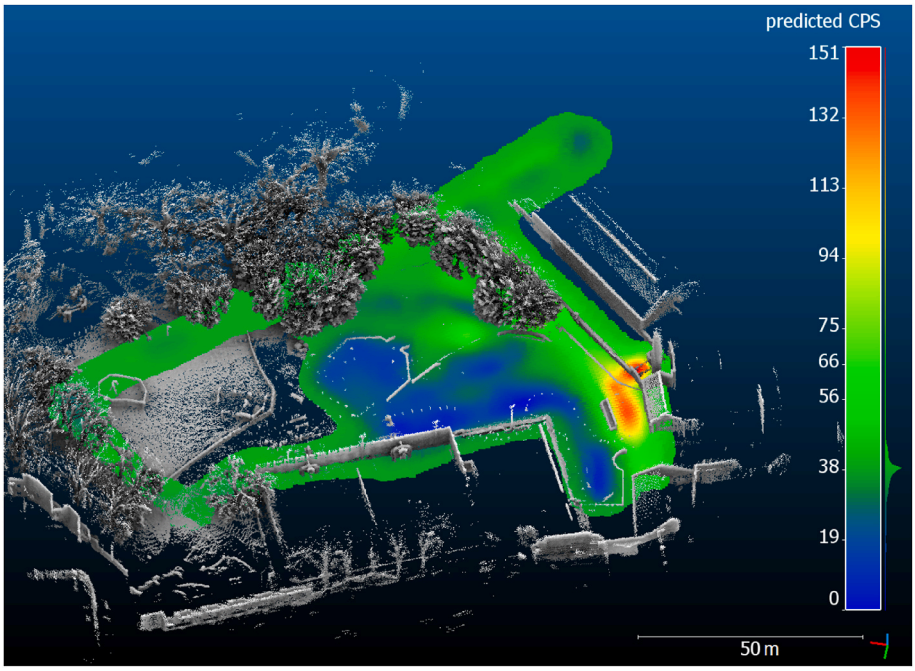

Fig. 5. Radiation map for Dame Emily Park, in which points have been interpolated using the Kriging method, as demonstrated in West et al. (2021).

energies and/or gamma yields they cannot be labelled with complete certainty.

As well as recording the overall variation in radiation intensity, the four Hamamatsu detectors also produced a gamma spectrum at each point during the survey. The gamma spectra recorded at the location highlighted in Fig. 3(b), where radiation intensity is at its highest, were summed to produce a combined gamma spectrum, with the gamma spectra recorded by the four Hamamatsu detectors exhibiting similar and corresponding results to those produced by the HPGe detector. However, minor photopeak's were more challenging to distinguish due to higher signal noise levels and lower energy resolution of the CsI(Tl) type Hamamatsu detectors.

Both samples recorded measurable radioactivity, primarily associated with K-40, but also with U-238 and Th-232. As all three radionuclides are naturally occurring and common constituents of fly ash, they were therefore expected to be present in the samples. The activity concentrations of K-40, U-238, and Th-232, determined via the HPGe system, can be seen in Table 1. From the table, the recorded activity concentrations of both U-238 and Th-232 fall below the adopted values of activity concentrations in escaping fly ash as reported by UNSCEAR (1982), and within the range of activity concentrations reported for collected fly ash by IAEA (1996). Any radionuclides that could not be

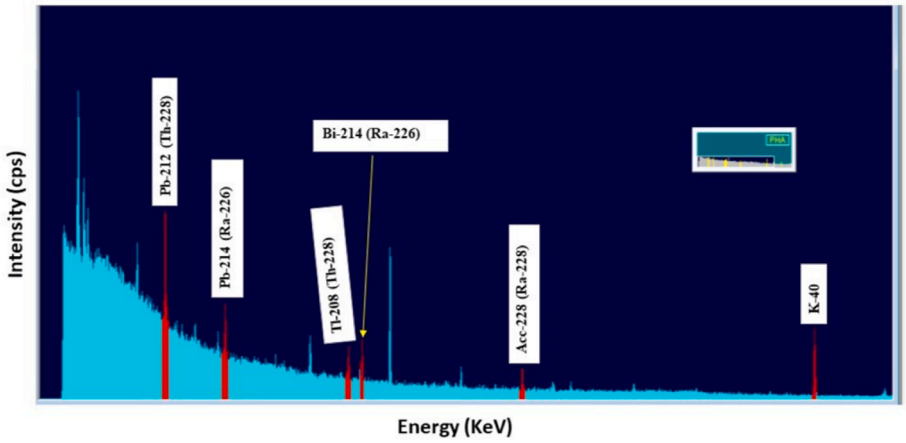

Fig. 6. Gamma-ray spectrum of sample C1.

Table 1
Measured activity concentrations for the two samples collected at the site (units are $Bqkg^{-1}$).

Sample	C1	C2
K-40	1,765 ± 75	1,610 ± 71
U-238	170 ± 9	180 ± 10
Th-232	170 ± 10	190 ± 11

labelled with certainty on the gamma spectra were discounted from activity concentration calculations. The relative error on each measurement is low.

5. Discussion

As reported, the amount of time required to comprehensively survey the site was limited (~60 min). However, a more detailed survey could have been produced had numerous different areas of elevated radioactivity been observed. The design of the system is such that batteries can be swapped whilst the system is in use, meaning the survey time could be extended indefinitely, if multiple batteries had been available. Surveying the site with the combined methodology for a longer duration would provide a denser point-cloud and therefore better coverage of the park. It would also reduce the reliance on interpolation to infer gamma radiation across large areas of the survey site. However, multiple runs of the site increased the coverage of both the point-cloud and gamma measurements. Interpolation via Kriging (West et al., 2021) also improved gamma coverage, creating estimates for areas not directly covered during the survey.

Activity concentrations of radionuclides in precursor coal from the Dean Lane colliery are unknown, and therefore direct comparisons between the two cannot be drawn. However, activities are heightened when compared with reported global average values for both coal and soils, indicating an enrichment of radionuclides during combustion. The 1982 report by the United Nations Scientific Committee on the Effects of Atomic Radiation (UNSCEAR) states average activity concentrations in unburnt coal to be 50 $Bqkg^{-1}$ for K-40 and 20 $Bqkg^{-1}$ for both U-238 and Th-232 (UNSCEAR, 1982). It must be noted that exceptions occur in certain cases. For example, where radionuclides are enriched, such as in uraniferous coals (UNSCEAR, 1982). Compared with these UNSCEAR values, activity concentrations in ground-truth sample C1 are 34 times higher for K-40, and 8 times higher for both U-238 and Th-232. Levels of enrichment are also similar in sample C2. However, the value of Annual Effective Dose Equivalent, AEDE (μSvy^{-1}) for C1 (313 μSvy^{-1}), and C2 (325 μSvy^{-1}) calculated following (El-Taher et al., 2009) were approximately eight times lower than the natural annual background effective dose of 2.4 mSv (UNSCEAR 2000).

The melting points of K-chloride and K-oxide are roughly 760 °C, far lower than the melting points of U and Th, whilst the melting points of K-feldspar and K-mica are roughly 1200 °C and 1300 °C respectively. Th and U can be explained in the fly ash samples, but K, and at such high activity concentrations is more difficult to justify. However, when considering temperatures experienced by coal during burning (exceeding that of 400–500 °C), it is possible that the secular equilibrium of U and Th-bearing micro-particulates was disturbed during heating. Hence, the assumptions used for the calculation of U-238 and Th-232 activity concentrations may be incorrect, and true U and Th activities could be much higher. To verify this, total acid dissolution of the samples followed by ultra-trace analysis mass-spectrometry should be conducted in a further study.

Although radon has not been directly detected on the produced gamma spectra, it can be inferred to be present, as a decay daughter of both U-238 and Th-232. Airborne radon, in high concentrations, presents significant health concerns on exposure, particularly when directly inhaled. In open spaces, radon exposure is of low concern, but inside colliery buildings with limited ventilation, the risks increase significantly. NORM detection is not limited to gamma surveys, and other decay particles, such as alpha particles can instead be measured. Remote alpha imaging measures the concentrations of alpha particles emitted from a surface using secondary 'conversion particles', in most cases nitrogen molecules (N_2) (Lamadie et al., 2005). Alpha particles interact with nitrogen molecules, creating ultraviolet (UV) photons, during a process called alpha-induced radioluminescence (Sand et al., 2015). This technology could therefore potentially be used inside the colliery chimney, in a dark environment, to produce distribution images of any alpha emitting materials such as U or Th-bearing particles. This would provide further understanding of the risks posed by the radionuclides present at the site.

Based on the data presented, there is no noteworthy radiological hazard associated with the former colliery site surveyed in this work. However, the technology deployed in this study clearly has the capability to detect small changes in the distribution and intensity of background radioactivity. This validation of sensitivity enables numerous different applications for the technology, varying from mine-site surveying to proving compliance with environmental regulations. It will also apply to mineral prospecting studies where NORMs are coincident with valuable minerals (Martin et al., 2020) and to rapid surveys of industrial sites which may have a legacy radiological footprint e.g., defunct mine sites, chemical processing plants and inactive coal-fired power stations awaiting decommissioning.

This technology would be highly complementary and integrable with drone-based survey techniques, including radiometric, LiDAR and

hyperspectral data collection. It is conceivable that the technology demonstrated herein, due to its light weight and compact size (<5 kg) could be deployed on a multi-rotor UAV flying at a low altitude to conduct site surveys where terrain is complex or not fully accessible by foot. Such a technology would also provide a valuable new tool to rapidly assess a site following a nuclear release incident, providing real-time data to emergency responders, which can inform subsequent clean-up activities.

6. Conclusions & future work

Overlaying the results of the gamma survey onto the produced 3D point-cloud has proved effective as a method of mapping radiation distribution. For a site of this scale, a ground-based survey has proved both efficient and effective. However, for similar studies covering larger or less accessible sites, the methodology can and must be adapted. For example, automating the survey so that both the LiDAR scanner and detectors are instead carried by a drone with the capability of carrying heavy payloads. Performing the survey with a drone would enable the vertical extent of buildings such as the chimney to be mapped. It would also assess the vertical distribution of gamma radiation, making the produced radiation distribution map 3-dimensional. However, whilst drones can cover larger areas, this comes at the cost of a decreased resolution.

This study has proven that although there is an area of elevated radioactivity proximal to the Dean Lane Colliery, radiation levels are low and do not pose a threat to the health of the general public. Radiation does not exceed 0.18 $\mu Svhr^{-1}$ across the entire site, and only exceeds 0.1 $\mu Svhr^{-1}$ at and immediately around the chimney building. Ground-truth samples were determined to exhibit activities consistent with published values, but are relatively enriched versus literature reports of activities in precursor coals. The elevated radioactivity can be inferred to be the direct result of coal combustion during mine operation. The residual exposure risk to the public is deemed to be very low and therefore the site is not of any immediate concern. However, care should be taken when removing waste products from sites such as this, as risks increase significantly when there is direct contact with mine tailings and fly ash. Appropriate PPE should be worn when entering the chimney infrastructure of the site, to eliminate the possibility of inhaling or becoming contaminated through contact with radioactive particulates.

Combining handheld and laboratory gamma spectrometry has provided useful and corresponding information on both the activity and signature of radiation at the site. Of increased concern are legacy mine sites in which there are direct pathways for radionuclides and toxic elements to enter waterways or the atmosphere. This also applies to sites, such as power stations, where fly ash particles can be easily re-suspended into the surrounding environment, putting the area immediately around the site at an increased risk. These sites should be prioritised for analysis similar to that reported in this study.

Declaration of competing interest

The authors declare no conflict of interest, financial or otherwise. The funders had no role in the design of the study; in the collection, analyses, or interpretation of data; in the writing of the manuscript, or in the decision to publish the results.

Data availability

A data DOI is now in the manuscript.

Acknowledgements

The authors would like to thank UK Research and Innovation (UKRI) and the Engineering and Physical Sciences Research Council (EPSRC) for their support and funding for this work via the Robotics and Artificial Intelligence for Nuclear (RAIN) Hub (EP/W001128/1) and NNUF-HR: National Nuclear User Facility for Hot Robotics (EP/T011491/1).

References

Bettey, J.H., 1978. The Rise of a Gentry Family: the Smyths of Ashton Court, C. 1500-1642, vol. 43. Bristol Branch of the Historical Association Local History Pamphlets, the University, Bristol.

CloudCompare, 2015. GPL software. version 2.6.1. https://www.cloudcompare.org/. (Accessed 1 March 2022).

Douet, J., 2016. Industrial Heritage Re-tooled: the TICCIH Guide to Industrial Heritage Conservation. Routledge.

Dowdall, M., Vicat, K., Frearson, I., Gerland, S., Lind, B., Shaw, G., 2004. Assessment of the radiological impacts of historical coal mining operations on the environment of Ny- Ålesund, Svalbard. J. Environ. Radioact. 71 (2), 101–114.

Eckert, Ziegler, 2007. Reference & calibration sources product information. Available at: https://www.ezag.com/fileadmin/user_upload/isotopes/isotopes/Isotrak/isotrak-pdf/Product_literature/EZIPL/EZIP_catalogue_reference_and_calibration_sources.pdf. (Accessed 18 July 2022).

Hamamatsu, 2020. C12137 series. Radiat. Detect. Modul. Available at: https://www.hamamatsu.com/content/dam/hamamatsu-photonics/sites/documents/99_SALES_LIBRARY/ssd/c12137_series_kacc1196e.pdf.

IAEA, 1996. Clearance Levels for Radionuclides in Solid Materials: Application of the Exemption Principles. Interim Report for Comment. IAEA TECDOC-855.

IAEA, 2019. Certified reference material IAEA – 385, natural and artificial radionuclides in sediment from the Irish sea. Available at: https://nucleus.iaea.org/sites/ReferenceMaterials/Shared%20Documents/ReferenceMaterials/Radionuclides/IAEA-385/RS_IAEA-385_V5.3.pdf. (Accessed 18 July 2022).

Lamadie, F., Delmas, F., Mahe, C., Girones, P., Le Goaller, C., Costes, J.R., 2005. Remote alpha imaging in nuclear installations: new results and prospects. IEEE Trans. Nucl. Sci. 52 (6), 3035–3039.

Lyes, J., 2002. Bristol 1901-1913. Bristol Branch Hist. Assoc. Local Hist. Pam. 104 (7759), 1362.

Martin, P.G., et al., 2020. Radiological identification of near-surface mineralogical deposits using low-altitude unmanned aerial vehicle. Rem. Sens. 12 (21), 3562.

Moore, L.R., Trueman, A.E., 1937. The coal measures of Bristol and Somerset. Q. J. Geol. Soc. 93 (1–4), 195–240.

Moore, L.R., Trueman, A.E., 1939. The structure of the Bristol and Somerset coalfield. Proc. Geol. Assoc. 50 (1), 46-IN4.

Okeme, I.C., Scott, T.B., Martin, P.G., Satou, Y., Ojonimi, T.I., Olaluwoye, M.O., 2020. Assessment of the mode of occurrence and radiological impact of radionuclides in Nigerian coal and resultant post-combustion coal ash using scanning electron microscopy and gamma-ray spectroscopy. Minerals 10 (3), 241.

Okeme, I.C., et al., 2021. An advanced analytical assessment of rare earth element concentration, distribution, speciation, crystallography and solid-state chemistry in fly ash. Spectrochim. Acta B Atom Spectrosc. 177, 105950.

Ordnance Survey, 2013a, 1844-1888 OS 25 1st Edition [Map], 1:2500. Available at: https://data.bristol.gov.uk/geonetwork/srv/eng/catalog.search#/metadata/d85151e3-c1da-4594-966a-72758490918a. (Accessed 1 August 2022).

Ordnance Survey, 2013b, 1947-1965 OS National Grid [Map], 1:2500. Available at: https://data.bristol.gov.uk/geonetwork/srv/eng/catalog.search#/metadata/a6450ac8-a200-41cf-9c73-c4b65516fc17. (Accessed 1 August 2022).

Ortec, 2020. Ortec, ametek – GEM series coaxial HPGe detector product configuration guide. Available at: https://www.ortec-online.com/-/media/ametekortec/brochures/g/gem.pdf?la=en&revision=85004f52-4b5d-4d62-8e27-e9ab1de89951. (Accessed 27 July 2022).

Ramezani, M., Wang, Y., Camurri, M., Wisth, D., Mattamala, M., Fallon, M., 2020. The newer college dataset: handheld lidar, inertial and vision with ground truth. In: 2020 IEEE/RSJ International Conference on Intelligent Robots and Systems (IROS). IEEE, pp. 4353–4360.

Ramsey, K., 2003. The Bristol coal industry. Bristol Branch Hist. Assoc. Local Hist. Pam. 106 (7759), 1362.

Ren, Z., Wang, L., Bi, L., 2019. Robust GICP-based 3D LiDAR SLAM for underground mining environment. Sensors 19 (13), 2915.

Sand, J., et al., 2015. Imaging of alpha emitters in a field environment. Nucl. Instrum. Methods Phys. Res. Sect. A Accel. Spectrom. Detect. Assoc. Equip. 782, 13–19.

Sun, Y., Qi, G., Lei, X., Xu, H., Wang, Y., 2016. Extraction of uranium in bottom ash derived from high-germanium coals. Procedia Environ. Sci. 31, 589–597.

Tian, Q., Guo, B., Nakama, S., Sasaki, 2018. Distributions and leaching behaviours of toxic elements in fly ash. ACS Omega 3 (10), 13055-1064.

United Nations Scientific Committee on the Effects of Atomic Radiation (UNSCEAR), 1982. *Ionizing Radiation: Sources and Biological Effects.* 1982 Report to the General Assembly, with Annexes. United States: United Nations.

Vetter, K., Barnowski, R., Cates, J.W., Haefner, A., Joshi, T.H., Pavlovsky, R., Quiter, B.J., 2019. Advances in nuclear radiation sensing: enabling 3-D gamma-ray vision. Sensors 19 (11), 2541.

West, A., Tsitsimpelis, I., Licata, M., Jazbec, A., Snoj, L., Joyce, M.J., Lennox, B., 2021. Use of Gaussian process regression for radiation mapping of a nuclear reactor with a mobile robot. Sci. Rep. 11 (1), 1–11.

Woodward, H.B., 1876. Geology of East Somerset and the Bristol Coal-Fields. HM Stationery Office. Memoirs of the Geological Survey - England and Wales.
World Nuclear Association (WNA), 2020. Naturally Occurring Radioactive Materials (NORM) [online]. Available at: https://www.world-nuclear.org/information-library/safety-and-security/radiation-and-health/naturally-occurring-radioactive-materials-norm.aspx. (Accessed 26 August 2022).
Zhao, J., Zhang, Z., Sullivan, C.J., 2019. Identifying anomalous nuclear radioactive sources using Poisson kriging and mobile sensor networks. PLoS One 14 (5), e0216131.